ELSEVIER

Polymer 43 (2002) 2549–2559

polymer

www.elsevier.com/locate/polymer

Development of molecular orientation and stress in biaxially deformed polymers. I. Affine deformation in a solid state

Leszek Jarecki*, Andrzej Ziabicki

Institute of Fundamental Technological Research, Polish Academy of Sciences, Swietokrzyska 21, 00-049 Warsaw, Poland

Received 2 July 2001; received in revised form 26 November 2001; accepted 26 November 2001

Abstract

Biaxial deformation of freely jointed chain molecules in a solid state is considered. Biaxial molecular orientation is directly related to the applied deformation. Segmental orientation and stress are considered using non-Gaussian inverse Langevin statistics of the chain end-to-end vectors. Padé approximation and series expansion of the inverse Langevin function are used.

Global orientation of chain segments and stress are analyzed for affine biaxial deformation of non-Gaussian chains. Molecular anisotropy is characterized by the norm of the average orientation tensor, $\|\mathbf{D}\|$, and the global anisotropy of the stress tensor is characterized by the norm $\|\mathbf{P}\|$. Non-linear behavior of the orientation vs. stress characteristics for isochoric uniaxial deformation, calendering ($\lambda_1 = 1$) and biaxial deformation are discussed. © 2002 Published by Elsevier Science Ltd.

Keywords: Biaxial orientation; Biaxial stress; Orientation

1. Introduction

Deformation of polymer systems composed of flexible chains leads to orientation of individual chain segments, affects free energy and stress. Molecular orientation is of considerable interest for uniaxially as well as biaxially deformed polymers, as related to mechanical behavior and structure. Stress-induced morphological transitions during biaxial (thermoforming, film blowing) or uniaxial deformation (fiber spinning) provide important components of process modeling.

We will consider systems of chain molecules subjected to biaxial deformation in a solid or fluid state. In a solid state, orientation produced by cold or hot drawing, thermoforming, etc. is controlled, first, by deformation applied to the material. Contribution of relaxation of the molecular orientation during deformation is much reduced due to deformation stresses transmitted in such systems to the chain ends in the case of crosslinked topology or strong viscous interactions in uncrosslinked systems. In a cross-linked, purely elastic system in a rubbery state, the extent of reversible deformation can be correlated with average orientation and anisotropy of physical properties. In the uncross-linked solids showing plastic behavior (e.g. strongly interacting polymer chains in the bulk) the deformation is irreversible, but frozen orientation is maintained long after deformation rate and stress are reduced to zero.

On the contrary, orientation produced in a viscous fluid (e.g. melt spinning, film blowing and film casting) is controlled by deformation rate or stress. In more complex, viscoelastic materials, effects of deformation and deformation rate are superimposed one on another. The comparison of orientation in Nylon 6 fibers, either cold-drawn in a plastic state (orientation controlled by draw ratio) or melt-spun (flow orientation controlled by spinning speed or spinning stress) [1] seem to confirm this picture. At the same time, melt spinning of highly viscoelastic polyethylene [2] reveals both, deformation (spin–draw ratio) and deformation rate (spinning speed) effects.

In the present paper, we will analyze the molecular orientation behavior of polymers subjected to isochoric, biaxial deformation in a solid state. Orientation in steady, viscous flow as well as in transient viscoelastic effects will be treated in separate papers.

Characterization and development of segmental orientation in flexible chain polymers subjected to biaxial deformation was investigated experimentally [3–15] and theoretically [5,7,12,16,17] by several authors. In theoretical studies of the orientation development, an assumption of finite extensibility of real chains is required, in particular at higher deformations. Nagai formulation [18], offering series expansion approach for the segmental orientation function in flexible chain polymers, was adopted for

* Corresponding author. Tel.: +48-22-827-8182; fax: +48-22-826-9815.
E-mail address: ljarecki@ippt.gov.pl (L. Jarecki).

0032-3861/02/$ - see front matter © 2002 Published by Elsevier Science Ltd.
PII: S0032-3861(02)00031-9

biaxial orientation in cross-linked systems by the authors [17]. The approach resulted in a series expansion theory of biaxial orientation in affinely deformed networks.

In our paper, we present a closed-formula theory for affinely deformed systems, based on Padé approximation of the inverse Langevin distribution of chain end-to-end vectors proposed by Cohen [19]. Series expansion formulation of the orientation characteristic, resulting from the expansion of the inverse Langevin function, is also presented.

2. Orientation and stress in a freely-jointed chain macromolecule

According to Kuhn and Grün [20], equilibrium distribution of end-to-end vectors, **h**, within a freely-jointed chain composed of N statistical Kuhn segments, reads

$$W_0(\mathbf{h}) = \text{const.}\exp\left(-\frac{F_{el}}{kT}\right) = \text{const.}\exp\left[-N\int_0^{h/Na}\mathscr{L}^*(x)\mathrm{d}x\right] \quad (1)$$

where F_{el} is the entropy-controlled elastic free energy of the chain, and a, the fixed length of the segment. $\mathscr{L}^*(x)$ is the inverse Langevin function which in the form of the series expansion reads

$$\mathscr{L}^*(x) = 3x + \frac{9}{5}x^3 + \frac{297}{175}x^5 + \frac{1539}{875}x^7 + \frac{126\,117}{67\,375}x^9 + \cdots \quad (2)$$

The expansion (2) converges slowly, in particular for $x > 1/2$. A (2,3) Padé approximation proposed by Cohen [19]

$$\mathscr{L}^*(x) = x\frac{3-x^2}{1-x^2} + \mathrm{O}(x^6) \quad (3)$$

offers a closed formula applicable in the entire range of the variable $x \in (0,1)$, including the asymptotic behavior

$$\lim_{x\to 0}\mathscr{L}^*(x) = 3x, \qquad \lim_{x\to 1}\mathscr{L}^*(x) = \frac{1}{1-x} \quad (4)$$

The end-to-end vectors' distribution

$$W_0(\mathbf{h}) = \text{const.}\exp\left\{-\frac{3h^2}{2Na^2}\left[1 + \frac{3}{10}\left(\frac{h}{Na}\right)^2 + \frac{33}{175}\left(\frac{h}{Na}\right)^4 + \frac{513}{3500}\left(\frac{h}{Na}\right)^6 + \frac{42\,039}{336\,875}\left(\frac{h}{Na}\right)^8 + \cdots\right]\right\} \quad (5)$$

reduces with the Padé approximation to

$$W_0(\mathbf{h}) \cong \text{const.}\left[1 - \left(\frac{h}{Na}\right)^2\right]^N \exp\left(-\frac{h^2}{2Na^2}\right) \quad (6)$$

The distribution W_0 for undeformed systems is spherically symmetric. External orienting forces applied to the system change this symmetry.

Orientation distribution of segments around the end-to-end vector **h** exhibits cylindrical symmetry, and is characterized by the function of the angle α between direction of the segment, **a**, and the vector **h** [21]

$$w_{s0}(\cos\alpha; h, N) = \frac{\mathscr{L}^*(h/Na)}{4\pi sh[\mathscr{L}^*(h/Na)]}\exp\left[\mathscr{L}^*\left(\frac{h}{Na}\right)\cos\alpha\right] \quad (7)$$

w_{s0} can be considered as the conditional probability of finding the segment with orientation α in the chain with end-to end distance h and the number of segments N.

In the range of small chain extensions, $h/Na \ll 1$, the distribution (7) reduces to

$$w_{s0}(\cos\alpha) \cong \frac{1}{4\pi}\exp\left(\frac{3h}{Na}\cos\alpha\right) \quad (8)$$

Orientation of segments within a single polymer chain is represented by the tensor [21]

$$\mathbf{A}(\mathbf{h}) = \left[1 - \frac{3\frac{h}{Na}}{\mathscr{L}^*\left(\frac{h}{Na}\right)}\right]\frac{\mathbf{h}\otimes\mathbf{h}}{h^2} = \left[\frac{3}{5}\left(\frac{h}{Na}\right)^2 + \frac{36}{175}\left(\frac{h}{Na}\right)^4 + \frac{108}{875}\left(\frac{h}{Na}\right)^6 + \frac{5508}{67\,375}\left(\frac{h}{Na}\right)^8 + \cdots\right]\frac{\mathbf{h}\otimes\mathbf{h}}{h^2} \quad (9)$$

which, in the limit of small extensions, $h/Na \ll 1$, reduces to

$$\mathbf{A}(\mathbf{h}) \cong \frac{3}{5}\frac{\mathbf{h}\otimes\mathbf{h}}{N^2a^2} \quad (10)$$

and with the Padé approximation, to

$$\mathbf{A}(\mathbf{h}) \cong \frac{2\mathbf{h}\otimes\mathbf{h}}{3N^2a^2 - h^2} \quad (11)$$

Note that in the range of small chain extensions, Eq. (11) does not reduce to Eq. (10), although both formulae assume zero values at zero end-to-end distance.

The number of chain configurations available at fixed end-to-end distance, h, is proportional to equilibrium distribution function, $W_0(\mathbf{h})$. The configurational entropy of the chain composed of N statistical segments reads

$$S(\mathbf{h}) = k\ln W_0(\mathbf{h}) = \text{Const} - Nk\int_0^{h/Na}\mathscr{L}^*(x)\mathrm{d}x \quad (12)$$

Substituting the expansion (2) in Eq. (12), chain entropy assumes the form

$$S(\mathbf{h}) = \text{Const} - \frac{3Nk}{2}\left[1 + \frac{3}{10}\left(\frac{h}{Na}\right)^2 + \frac{33}{175}\left(\frac{h}{Na}\right)^4 + \frac{513}{3500}\left(\frac{h}{Na}\right)^6 + \frac{42\,039}{336\,875}\left(\frac{h}{Na}\right)^8 + \cdots\right]\left(\frac{h}{Na}\right)^2 \quad (13)$$

which for the small extension, $h/Na \ll 1$, reduces to

$$S(\mathbf{h}) \cong \text{Const} - \frac{3Nk}{2}\left(\frac{h}{Na}\right)^2 \tag{14}$$

and with the Padé formula to

$$S(\mathbf{h}) \cong \text{Const} - Nk\left[\frac{1}{2}\left(\frac{h}{Na}\right)^2 - \ln\left(1-\left(\frac{h}{Na}\right)^2\right)\right] \tag{15}$$

It is evident that for $h/Na \ll 1$ Eq. (15) converges to the Gaussian limit (14).

The elastic tension **f** between chain ends is collinear with the end-to-end vector **h** and results as a gradient of the entropy-controlled elastic free energy

$$\mathbf{f} = \nabla F_{\text{el}}(\mathbf{h}) = -T\nabla S(\mathbf{h}) = \frac{kT}{a}\mathscr{L}^*\left(\frac{h}{Na}\right)\frac{\mathbf{h}}{h} \tag{16}$$

The corresponding local stress tensor reads

$$\mathbf{p} = \frac{1}{Nv_0}\mathbf{f}\otimes\mathbf{h} = \frac{\mathrm{kT}}{v_0}\left(\frac{h}{Na}\right)\mathscr{L}^*\left(\frac{h}{Na}\right)\frac{\mathbf{h}\otimes\mathbf{h}}{h^2} \tag{17}$$

where v_0 denotes the molecular volume of a single segment, and Nv_0, the volume of a polymer chain. Using the expansion formula (2) one obtains (from Eqs. (16) and (17))

$$\mathbf{f}(\mathbf{h}) = 3kT\left[1 + \frac{3}{5}\left(\frac{h}{Na}\right)^2 + \frac{99}{175}\left(\frac{h}{Na}\right)^4 + \frac{513}{875}\left(\frac{h}{Na}\right)^6 + \frac{42\,039}{67\,375}\left(\frac{h}{Na}\right)^8 + \cdots\right]\frac{\mathbf{h}}{Na^2} \tag{18}$$

$$\mathbf{p}(\mathbf{h}) = \frac{3kT}{Nv_0}\left[1 + \frac{3}{5}\left(\frac{h}{Na}\right)^2 + \frac{99}{175}\left(\frac{h}{Na}\right)^4 + \frac{513}{875}\left(\frac{h}{Na}\right)^6 + \frac{42\,039}{67\,375}\left(\frac{h}{Na}\right)^8 + \cdots\right]\frac{\mathbf{h}\otimes\mathbf{h}}{Na^2} \tag{19}$$

In the limit of small deformations, Eq. (18) reduces to the harmonic potential force between chain ends. Then, the corresponding stress tensor reads

$$\mathbf{p} = \frac{3kT}{v_0}\frac{\mathbf{h}\otimes\mathbf{h}}{N^2a^2} \tag{20}$$

In the Padé approximation, the stress tensor assumes the following form

$$\mathbf{p} \cong \frac{kT}{v_0}\left[\frac{3-\left(\frac{h}{Na}\right)^2}{1-\left(\frac{h}{Na}\right)^2}\right]\frac{\mathbf{h}\otimes\mathbf{h}}{N^2a^2} \tag{21}$$

Molecular orientation and stress tensors are coaxial, and can be considered as functions of a single dyadic variable, $\mathbf{h}\otimes\mathbf{h}$. It should be reminded that all powers of a dyadic are coaxial

$$(\mathbf{h}\otimes\mathbf{h})^n = h^{2(n-1)}\mathbf{h}\otimes\mathbf{h} \tag{22}$$

and the orientation and stress tensors can be expanded in power series of the dyadic $\mathbf{h}\otimes\mathbf{h}$

$$\mathbf{A}(\mathbf{h}) = \frac{3}{5}\frac{\mathbf{h}\otimes\mathbf{h}}{N^2a^2} + \frac{36}{175}\left(\frac{\mathbf{h}\otimes\mathbf{h}}{N^2a^2}\right)^2 + \frac{108}{875}\left(\frac{\mathbf{h}\otimes\mathbf{h}}{N^2a^2}\right)^3 + \frac{5508}{67\,375}\left(\frac{\mathbf{h}\otimes\mathbf{h}}{N^2a^2}\right)^4 + \cdots = \frac{3}{5}\frac{\mathbf{h}\otimes\mathbf{h}}{N^2a^2}\left[1 + \frac{12}{35}\left(\frac{h}{Na}\right)^2 + \frac{36}{175}\left(\frac{h}{Na}\right)^4 + \frac{1836}{13\,493}\left(\frac{h}{Na}\right)^6 + \cdots\right] \tag{23}$$

$$\mathbf{p}(\mathbf{h}) = \frac{3kT}{v_0}\left[\frac{\mathbf{h}\otimes\mathbf{h}}{N^2a^2} + \frac{3}{5}\left(\frac{\mathbf{h}\otimes\mathbf{h}}{N^2a^2}\right)^2 + \frac{99}{175}\left(\frac{\mathbf{h}\otimes\mathbf{h}}{N^2a^2}\right)^3 + \frac{513}{875}\left(\frac{\mathbf{h}\otimes\mathbf{h}}{N^2a^2}\right)^4 + \frac{42\,039}{67\,375}\left(\frac{\mathbf{h}\otimes\mathbf{h}}{N^2a^2}\right)^5 + \cdots\right] = \frac{3kT}{v_0}\frac{\mathbf{h}\otimes\mathbf{h}}{N^2a^2}\left[1 + \frac{3}{5}\left(\frac{h}{Na}\right)^2 + \frac{99}{175}\left(\frac{h}{Na}\right)^4 + \frac{513}{875}\left(\frac{h}{Na}\right)^6 + \frac{42\,039}{67\,375}\left(\frac{h}{Na}\right)^8 + \cdots\right] \tag{24}$$

Alternatively, the orientation tensor can be expanded in power series of the dimensionless stress, $(\mathbf{p}v_0/kT)$

$$\mathbf{A}(\mathbf{p}) = \frac{1}{5}\frac{\mathbf{p}v_0}{kT} - \frac{3}{175}\left(\frac{\mathbf{p}v_0}{kT}\right)^2 - \frac{1}{875}\left(\frac{\mathbf{p}v_0}{kT}\right)^3 + \frac{13}{67\,375}\left(\frac{\mathbf{p}v_0}{kT}\right)^4 + \cdots \tag{25}$$

and vice versa

$$\mathbf{p}(\mathbf{A}) = 5\frac{kT}{v_0}\left(\mathbf{A} + \frac{3}{7}\mathbf{A}^2 + \frac{25}{49}\mathbf{A}^3 + \frac{2125}{3773}\mathbf{A}^4 + \cdots\right) \tag{26}$$

For the Gaussian limit, linear relation known as 'stress-optical' or 'elastooptical' law is obtained

$$\mathbf{A}(\mathbf{p}) \cong \frac{1}{5}\frac{v_0\mathbf{p}}{kT} \tag{27}$$

3. A system of deformed macromolecules

From the distribution of chain end-to-end vectors, one can predict the global orientation distribution of chain segments in the system, $w_s(\theta,\varphi)$. Integration of the distribution of segments within a single chain, $w_{s0}(\alpha)$, with the normalized distribution of end-to-end vectors, $W(\mathbf{h})$, yields global orientation distribution of chain segments in the system

$$w_s(\theta,\varphi) = \int\int\int w_{s0}(\alpha)W(\mathbf{h})\mathrm{d}^3\mathbf{h} \tag{28}$$

where $\cos\alpha = \mathbf{a}\cdot\mathbf{h}/(ah)$ is defined by the scalar product of the segment vector, **a**, and the end-to-end vector, **h**. θ, φ

denote the polar angles in an external coordinate system. The global orientation distribution of segments is normalized in the rotational space

$$\int\int w_s(\theta,\varphi)\sin\theta\,d\theta\,d\varphi = 1 \tag{29}$$

At a given moment of time, t, the distribution function $W(h,t)$ can be found from the continuity equation

$$\frac{\partial W}{\partial t} + \mathrm{div}\left[W\dot{\mathbf{h}}_0 - D\left(\nabla W + W\nabla\frac{F_{el}}{kT}\right)\right] = 0 \tag{30}$$

where D is the diffusion coefficient, and $F_{el}(\mathbf{h})$, is the elastic free energy of the chain. The gradient and divergence operators concern the **h**-space. The *convective velocity* of the end-to-end vector, $\dot{\mathbf{h}}_0$, is related to flow characterized by the imposed flow (deformation rate) tensor, **Q**

$$\dot{\mathbf{h}}_0 = \mathbf{Q}\cdot\mathbf{h} \tag{31}$$

$$\mathbf{Q} = \frac{1}{2}(\nabla\mathbf{V} + \nabla\mathbf{V}^{T}) \tag{32}$$

$$\mathbf{Q} = \nabla\mathbf{V} = \begin{bmatrix} q_1 & 0 & 0 \\ 0 & q_2 & 0 \\ 0 & 0 & q_3 \end{bmatrix}, \qquad \|\mathbf{Q}\| = (\mathrm{tr}\,\mathbf{Q})^{1/2} = (q_1+q_2+q_3)^{1/2} \tag{33}$$

where the axial velocity gradients q_i are also the axial deformation rates. For isochoric deformation we have $\mathrm{tr}\,\mathbf{Q} = q_1 + q_2 + q_3 = 0$.

Several solutions of the continuity Eq. (30) deserve discussion. In the present paper, we analyze the effects of *affine* deformation of chains in the solid state. In the rubbery state, the affinity of deformation of chain end-to-end vectors is a characteristic feature of the Gaussian network. Application to non-Gaussian rubbery system can be considered as an approximation. In an uncross-linked system, affine deformation results from Eq. (30) as an asymptotic solution at zero diffusion coefficient (infinite interchain friction coefficient, see Section 4).

We should realize that for a fraction of chains with higher end-to-end distances in the initial distribution, affine deformation leads to end-to-end distances exceeding the chain contour length. Fraction of such chains is higher, and the affinity assumption is coarser, for higher deformations. Nevertheless, an upper limit of validity of affine deformation assumption is considered in terms of deformation of a chain with average dimensions. For a biaxial deformation, the upper bound for affinity is defined from the condition of full extension of a chain with an average end-to-end distance $\langle h^2\rangle_0^{1/2}$ in the initial state of the system [17]. Other deviations from affinity may result from the non-Gaussian chain behavior in crosslinked systems at equilibrium.

In the case of uncross-linked solids, affine deformation is obtained in Section 4 as a direct consequence of very high interchain friction forces and viscosity from the continuity equation in the limit of zero diffusion coefficient, at finite intrachain elastic force. Very high viscous interactions may concern also shorter parts of chain macromolecules and, in consequence, the assumption of affine deformation concerns shorter length scale than the chain end-to-end distance. But in such a case affine deformation of the chain portions results in affine deformation of the end-to-end vector of the entire chain macromolecule.

4. Distribution of polymer chains in a deformed uncross-linked solid

Consider a system with a very low molecular mobility. This is realized by strong intermolecular interactions which create sort of a plastic medium with infinitely high viscosity. Dividing Eq. (30) term-wise by the scalar measure of the deformation rate tensor $\|\mathbf{Q}\|$, in the limit $D/\|\mathbf{Q}\| \to 0$ we obtain the first order differential equation

$$\frac{\partial W}{\partial t} + W\,\mathrm{tr}\,\mathbf{Q} + (\mathbf{Q}\cdot\mathbf{h})\cdot\nabla W = 0 \tag{34}$$

Solution of Eq. (34), with the initial condition given by the unperturbed equilibrium distribution

$$W(\mathbf{h}, t=0) = W_0(\mathbf{h}) \tag{35}$$

can be presented in the form

$$W(\mathbf{h},t) = \exp[-\mathrm{tr}(\mathbf{Q}t)]W_0[\exp(-\mathbf{Q}t)\cdot\mathbf{h}] \tag{36}$$

The above solution is equivalent to the assumption that all end-to-end vectors in the initial sample, $\mathbf{h}(t=0)$, are subjected to affine (linear) transformation with the same time-dependent displacement gradient tensor $\mathbf{\Lambda}(t)$

$$\mathbf{h}(t) = \mathbf{\Lambda}(t)\cdot\mathbf{h}(t=0) \tag{37}$$

Affinity of deformation results from the fact that chains are convected by uniform flow field in a diffusion-free medium. At the same time, the affinity does not depend on whether the chains are Gaussian or not.

The deformation gradient tensor corresponding to diagonal deformation rate tensor is also diagonal and reads

$$\mathbf{\Lambda}(t) = \exp(\mathbf{Q}t) = \begin{bmatrix} \lambda_1(t) & 0 & 0 \\ 0 & \lambda_2(t) & 0 \\ 0 & 0 & \lambda_3(t) \end{bmatrix} \tag{38}$$

where the time-dependent components

$$\lambda_i(t) = \exp(q_i t) \tag{39}$$

The distribution of chain end-to-end vectors in the deformed sample can be expressed in terms of the time-dependent

deformation tensor

$$\mathbf{\Gamma}(t) = \mathbf{\Lambda}^{\mathrm{T}}(t)\mathbf{\Lambda}(t) = \begin{bmatrix} \lambda_1^2(t) & 0 & 0 \\ 0 & \lambda_2^2(t) & 0 \\ 0 & 0 & \lambda_3^2(t) \end{bmatrix} \tag{40}$$

which yields

$$W(\mathbf{h}, \mathbf{\Gamma}) = (\det \mathbf{\Gamma})^{-1/2} W_0(\mathbf{h}\cdot\mathbf{\Gamma}^{-1}\mathbf{h}) \tag{41}$$

For isochoric deformation we have $\det \mathbf{\Gamma}(t) = \det[\exp(\mathrm{tr}\, \mathbf{Q}t)] = 1$.

Using inverse Langevin form of the initial distribution $W_0(\mathbf{h})$, we obtain

$$W(\mathbf{h}, \mathbf{\Gamma}) = \text{const.}(\det \mathbf{\Gamma})^{-1/2} \exp\left[-N \int_0^{(\mathbf{h}\cdot\mathbf{\Gamma}^{-1}\mathbf{h})^{1/2}/Na} \mathscr{L}^*(x)\mathrm{d}x \right] \tag{42}$$

with the normalization condition

$$\int\int\int W(\mathbf{h}, \mathbf{\Gamma})\mathrm{d}^3\mathbf{h} = 1 \tag{43}$$

With the series expansion, Eq. (2), we obtain

$$W(\mathbf{h}, \mathbf{\Gamma}) = \text{const.}(\det \mathbf{\Gamma})^{-1/2} \exp\left\{ -\frac{3}{2}\frac{\mathbf{h}\cdot\mathbf{\Gamma}^{-1}\mathbf{h}}{Na^2} \times \left[1 + \frac{3}{10}\frac{\mathbf{h}\cdot\mathbf{\Gamma}^{-1}\mathbf{h}}{N^2a^2} + \frac{33}{175}\left(\frac{\mathbf{h}\cdot\mathbf{\Gamma}^{-1}\mathbf{h}}{N^2a^2}\right)^2 + \frac{513}{3500}\left(\frac{\mathbf{h}\cdot\mathbf{\Gamma}^{-1}\mathbf{h}}{N^2a^2}\right)^3 + \frac{42\,039}{336\,875}\left(\frac{\mathbf{h}\cdot\mathbf{\Gamma}^{-1}\mathbf{h}}{N^2a^2}\right)^4 + \cdots \right] \right. \tag{44}$$

In the range of small deformations, Eq. (44) reduces to the deformed Gaussian distribution

$$W(\mathbf{h}, \mathbf{\Gamma}) \cong (\det \mathit{\Gamma})^{-1/2} \left(\frac{3}{2\pi Na^2}\right)^{3/2} \exp\left(-\frac{3}{2}\frac{\mathbf{h}\cdot\mathbf{\Gamma}^{-1}\mathbf{h}}{Na^2} \right) \tag{45}$$

and, in the non-linear range with the Padè approximation

$$W(\mathbf{h}, \mathbf{\Gamma}) \cong \text{const.}(\det \mathbf{\Gamma})^{-1/2} \times \left(1 - \frac{\mathbf{h}\cdot\mathbf{\Gamma}^{-1}\mathbf{h}}{N^2a^2} \right)^N \exp\left(-\frac{1}{2}\frac{\mathbf{h}\cdot\mathbf{\Gamma}^{-1}\mathbf{h}}{Na^2} \right) \tag{46}$$

Orientation distribution of chain segments in the system subjected to deformation $\mathbf{\Gamma}$ is obtained from the integral (28) with the appropriate forms of $W(\mathbf{h})$ and $w_{s0}(\alpha)$. Using linearized orientation distribution function (Eq. (8)) and the deformed Gaussian form of the distribution of end-to-end vectors $\mathbf{h}$ (Eq. (45)) one obtains

$$w_s(\theta, \varphi) \cong \frac{1}{4\pi}\exp\left(\frac{3}{2}\frac{\mathbf{a}\cdot\mathbf{\Gamma}\mathbf{a}}{Na^2} \right) \tag{47}$$

θ and φ are polar angles of the segment vector $\mathbf{a}$ in an external coordinate system

$$\mathbf{a} = a\begin{bmatrix} \sin\theta\cos\varphi \\ \sin\theta\sin\varphi \\ \cos\theta \end{bmatrix} \tag{48}$$

Orientation-dependent exponent in Eq. (47) assumes the form

$$\frac{\mathbf{a}\cdot\mathbf{\Gamma}\mathbf{a}}{a^2} = \left(\lambda_1^2\cos^2\varphi + \lambda_2^2\sin^2\varphi\right)\sin^2\theta + \lambda_3^2\cos^2\theta \tag{49}$$

5. Average behavior of deformed systems

To characterize the behavior of a system of chains subjected to deformation, single chain characteristics such as entropy, $S(\mathbf{h})$, orientation tensor, $\mathbf{A}(\mathbf{h})$, and stress tensor, $\mathbf{p}(\mathbf{h})$, should be averaged with actual distribution $W(\mathbf{h})$ of the end-to-end vectors. Average entropy, average orientation and stress tensors are calculated from the integrals

$$\langle S\rangle = \int\int\int S(\mathbf{h})W(\mathbf{h})\mathrm{d}^3\mathbf{h} \tag{50}$$

$$\langle \mathbf{A}\rangle = \int\int\int \mathbf{A}(\mathbf{h})W(\mathbf{h})\mathrm{d}^3\mathbf{h} \tag{51}$$

$$\langle \mathbf{p}\rangle = \int\int\int \mathbf{p}(\mathbf{h})W(\mathbf{h})\mathrm{d}^3\mathbf{h} \tag{52}$$

Even moments of the end-to-end distance are obtained by integration with the appropriate distribution, $W(\mathbf{h})$

$$\langle h^{2n}\rangle = \int h^{2n}W(\mathbf{h})\mathrm{d}^3\mathbf{h} \tag{53}$$

The average end-to-end vector $\mathbf{h}$, and force $\mathbf{f}$, multiplied by even powers of the end-to-end distance disappear

$$\langle h^{2n}\mathbf{h}\rangle = \langle h^{2n}\mathbf{f}\rangle = 0 \tag{54}$$

and the average dyadics are obtained in the form

$$\langle h^{2n}\mathbf{h}\otimes\mathbf{h}\rangle = \int h^{2n}\mathbf{h}\otimes\mathbf{h}W(\mathbf{h})\mathrm{d}^3\mathbf{h} \tag{55}$$

Using the 'deformed' distribution Eq. (41), the average entropy per chain segment for an isochoric deformation, $\det \mathbf{\Gamma} = 1$, results in the form

$$\frac{\langle S\rangle}{kN} = \text{Const} - \frac{1}{2}\mathrm{tr}\left(\frac{\mathbf{\Gamma}}{N}\right) - \frac{1}{20}\left[2\,\mathrm{tr}\left(\frac{\mathbf{\Gamma}}{N}\right)^2 + \left(\mathrm{tr}\left(\frac{\mathbf{\Gamma}}{N}\right)\right)^2 \right] - \mathrm{O}\left(\frac{\mathbf{\Gamma}}{N}\right)^3 \tag{56}$$

and the average orientation and stress tensors:

$$\langle \mathbf{A} \rangle = \frac{1}{5}\frac{\mathbf{\Gamma}}{N} + \frac{4}{175}\left[2\left(\frac{\mathbf{\Gamma}}{N}\right)^2 + \frac{\mathbf{\Gamma}}{N}\mathrm{tr}\left(\frac{\mathbf{\Gamma}}{N}\right)\right] + \mathrm{O}\left(\frac{\mathbf{\Gamma}}{N}\right)^3 \tag{57}$$

$$\frac{\langle \mathbf{p} \rangle v_0}{kT} = \frac{\mathbf{\Gamma}_1}{N} + \frac{1}{5}\left[2\left(\frac{\mathbf{\Gamma}}{N}\right)^2 + \frac{\mathbf{\Gamma}}{N}\mathrm{tr}\left(\frac{\mathbf{\Gamma}}{N}\right)\right] + \mathrm{O}\left(\frac{\mathbf{\Gamma}}{N}\right)^3 \tag{58}$$

The average characteristics are expressed in terms of the affine deformation tensor reduced by the number of statistical segments within a chain, $\mathbf{\Gamma}/N$. The respective deformation components, λ_i^2/N, characterize *effective molecular deformation*.

Eqs. (57) and (58) indicate that the average stress and orientation tensors are collinear only in the first order (linear) approximation.

Anisotropy of the system is characterized by the deviator of the average orientation tensor, each principal component of which, f_i, describes the molecular orientation in the direction of the ith axis

$$\mathbf{D} = \mathrm{dev}\langle \mathbf{A} \rangle = \langle \mathbf{A} \rangle - \frac{1}{3}\mathrm{tr}\langle \mathbf{A} \rangle \mathbf{I} = \frac{2}{3}\begin{bmatrix} f_1 & 0 & 0 \\ 0 & f_2 & 0 \\ 0 & 0 & f_3 \end{bmatrix} \tag{59}$$

The principal orientation factors read

$$\begin{aligned} f_1 &= \langle A_{11} \rangle - \frac{1}{2}(\langle A_{22} \rangle + \langle A_{33} \rangle) \\ f_2 &= \langle A_{22} \rangle - \frac{1}{2}(\langle A_{11} \rangle + \langle A_{33} \rangle) \\ f_3 &= \langle A_{33} \rangle - \frac{1}{2}(\langle A_{11} \rangle + \langle A_{22} \rangle) \end{aligned} \tag{60}$$

From the definition of the deviator it follows that

$$f_1 + f_2 + f_3 = 0 \tag{61}$$

The norm of tensor $\mathbf{D}$

$$\|\mathbf{D}\| = [\mathrm{tr}(\mathbf{D}\mathbf{D}^{\mathrm{T}})]^{1/2} = \frac{2}{3}\left(f_1^2 + f_2^2 + f_3^2\right)^{1/2} \tag{62}$$

is a measure of the system *global anisotropy*.

Similarly, the norm of the deviator of average stress tensor

$$\mathbf{P} = \mathrm{dev}\langle \mathbf{p} \rangle = \langle \mathbf{p} \rangle - \frac{1}{3}\mathrm{tr}\langle \mathbf{p} \rangle \cdot \mathbf{I} \tag{63}$$

reads

$$\begin{aligned} \|\mathbf{P}\| &= [\mathrm{tr}(\mathbf{P}\mathbf{P}^{\mathrm{T}})]^{1/2} = \mathrm{tr}(\langle \mathbf{p} \rangle^2) - \frac{1}{3}(\mathrm{tr}\langle \mathbf{p} \rangle)^2 \\ &= \left[\frac{2}{3}\left(\langle p_{11} \rangle^2 + \langle p_{22} \rangle^2 + \langle p_{33} \rangle^2 \right.\right. \\ &\quad \left.\left. - \langle p_{11} \rangle\langle p_{22} \rangle - \langle p_{11} \rangle\langle p_{33} \rangle - \langle p_{22} \rangle\langle p_{33} \rangle \right)\right]^{1/2} \end{aligned} \tag{64}$$

and characterizes the intensity of anisotropic stress in the system. $\|\mathbf{P}\|$ disappears for a purely hydrostatic stress $\langle p_{11} \rangle = \langle p_{22} \rangle = \langle p_{33} \rangle$.

6. Discussion

We will consider isochoric, biaxial deformation with components

$$\lambda_1 > 0, \quad \lambda_3 > 0, \quad \lambda_2 = \frac{1}{\lambda_1\lambda_3}; \quad \lambda_1\lambda_2\lambda_3 = 1 \tag{65}$$

which in the uniaxial case reduces to

$$\lambda_1 = \lambda_2 = \frac{1}{(\lambda_3)^{1/2}} \tag{66}$$

The average entropy per a single chain segment, expressed by the deformation components, assumes the form

$$\begin{aligned} \frac{\langle S \rangle}{N} &= \mathrm{Const} - \frac{k}{2N}\left(\lambda_1^2 + \lambda_3^2 + \frac{1}{\lambda_1^2\lambda_3^2} \right) - \frac{3k}{20N^2} \\ &\quad \times \left[\lambda_1^4 + \lambda_3^4 + \frac{1}{\lambda_1^4\lambda_3^4} + \frac{2}{3}\left(\lambda_1^2\lambda_3^2 + \frac{1}{\lambda_1^2} + \frac{1}{\lambda_3^2} \right)\right] \\ &\quad - \mathrm{O}\left(\frac{1}{N^3}\right) \end{aligned} \tag{67}$$

for isochoric biaxial deformation, and

$$\begin{aligned} \frac{\langle S \rangle}{N} &= \mathrm{Const.} - \frac{k}{2N}\left(\lambda_3^2 + \frac{2}{\lambda_3} \right) \\ &\quad - \frac{3k}{20N^2}\left[3\lambda_3^4 + \frac{8}{\lambda_3^2} + 4\lambda_3 \right] - \mathrm{O}\left(\frac{1}{N^3}\right) \end{aligned} \tag{68}$$

for the isochoric uniaxial case.

The orientation factors for biaxial deformation read

$$\begin{aligned} f_1 &= \frac{1}{5N}\left[\lambda_1^2 - \frac{1}{2}\left(\lambda_3^2 + \frac{1}{\lambda_1^2\lambda_3^2} \right)\right] + \frac{8}{175N^2} \\ &\quad \times \left\{ \lambda_1^4 - \frac{1}{2}\left(\lambda_3^4 + \frac{1}{\lambda_1^4\lambda_3^4} \right) + \frac{1}{2}\left(\lambda_1^2 + \lambda_3^2 + \frac{1}{\lambda_1^2\lambda_3^2} \right) \right. \\ &\quad \left. \times \left[\lambda_1^2 - \frac{1}{2}\left(\lambda_3^2 + \frac{1}{\lambda_1^2\lambda_3^2} \right)\right]\right\} + \mathrm{O}\left(\frac{1}{N^3}\right) \end{aligned} \tag{69}$$

$$\begin{aligned} f_3 &= \frac{1}{5N}\left[\lambda_3^2 - \frac{1}{2}\left(\lambda_1^2 + \frac{1}{\lambda_1^2\lambda_3^2} \right)\right] + \frac{8}{175N^2} \\ &\quad \times \left\{ \lambda_3^4 - \frac{1}{2}\left(\lambda_1^4 + \frac{1}{\lambda_1^4\lambda_3^4} \right) + \frac{1}{2}\left(\lambda_1^2 + \lambda_3^2 + \frac{1}{\lambda_1^2\lambda_3^2} \right) \right. \\ &\quad \left. \times \left[\lambda_3^2 - \frac{1}{2}\left(\lambda_1^2 + \frac{1}{\lambda_1^2\lambda_3^2} \right)\right]\right\} + \mathrm{O}\left(\frac{1}{N^3}\right) \end{aligned} \tag{70}$$

$$f_2 = -(f_1 + f_3) \tag{71}$$

and for the uniaxial case, reduce to

$$f_3 = \frac{1}{5N}\left(\lambda_3^2 - \frac{1}{\lambda_3}\right) + \frac{4}{175N^2}\left(3\lambda_3^4 + \lambda_3 - \frac{4}{\lambda_3}\right) + \mathrm{O}\left(\frac{1}{N^3}\right) \tag{72}$$

$$f_1 = f_2 = -\frac{1}{2}f_3 \tag{73}$$

The first (Gaussian) term in Eq. (70), yields for the orientation factor f_3

$$f_3 = \frac{1}{5N}\left[\lambda_3^2 - \frac{1}{2}\left(\lambda_1^2 + \frac{1}{\lambda_1^2\lambda_3^2}\right)\right] \tag{74}$$

Behavior of the axial orientation factors f_1 and f_3 vs. elongation ratio λ_3, at fixed values of the elongation ratio λ_1 is shown in Figs. 1 and 2 for the system of non-Gaussian chains subjected to isochoric, affine biaxial stretch. Stretch ratios smaller than unity correspond to compression. The plots are computed from the terms in Eq. (60) for chains composed of $N = 100$ segments. Non-Gaussian distribution of end-to-end vectors, Eq. (42), is used for the averaging together with the Padé approximation of the inverse Langevin function, Eq. (3).

The integration is performed within the range of physically allowed extensions of the chains. At full extension, $h/Na = 1$, we have infinite values of the inverse Langevin function, of its Padè approximation, and the retractive elastic force between the chain ends tends to infinity. We introduce an ϵ margin which prevents the ratio h/Na from approaching unity and eliminates the singularity from our computations. We choose $\epsilon = 0.001$, a value which, on one side, eliminates computational singularities, and affects the results negligibly on the other. The chain full extension is reduced to a slightly smaller value of $h/Na = 1 - \epsilon =$ 0.999. Other chains in the system, which do not approach full extension, follow the scheme of affine deformation. We should note that such a picture of affine deformation applies for the deformation range determined by full extension of an average chain, with end-to-end-distance equal to $\langle h^2\rangle_0^{1/2}$ in the unperturbed system. Then, our computations for the system of chains composed of $N = 100$ statistical segments apply for $\lambda_1^2 + \lambda_3^2 + 1/(\lambda_1\lambda_3)^2 \le 100$. The inequality defines the physical range of deformation.

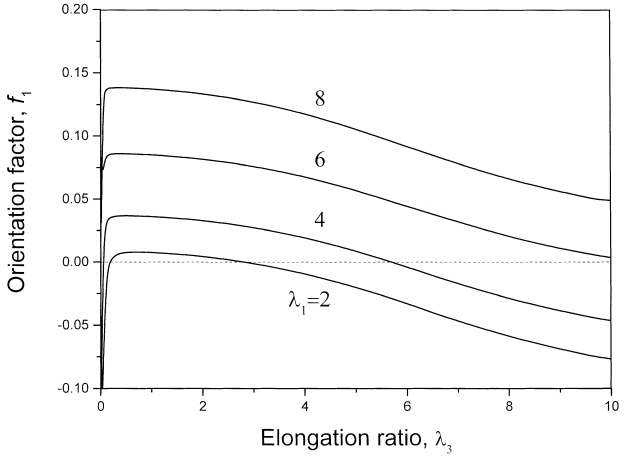

Fig. 1. Axial orientation factor f_1 vs. elongation ratio λ_3, at fixed values of the elongation ratio λ_1 (indicated), computed from Eq. (60) for biaxial affine deformation of non-Gaussian chains with the distribution of end-to-end vectors given by Eq. (42), and Padé approximation for the inverse Langevin function, $N = 100$.

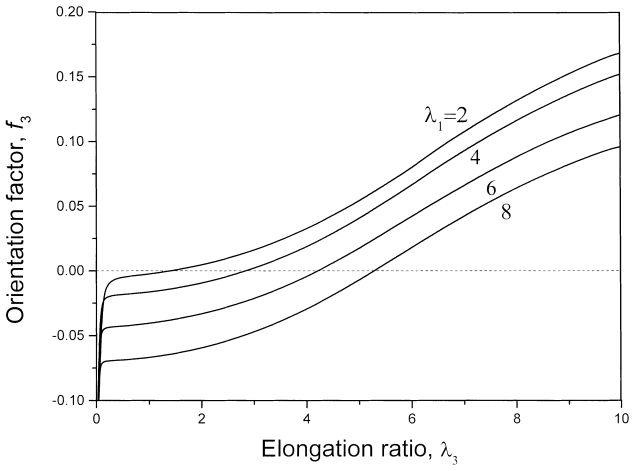

Fig. 2. Axial orientation factor f_3 vs. elongation ratio λ_3, at fixed values of the elongation ratio λ_1 (indicated) computed from Eq. (60) for biaxial affine deformation of non-Gaussian chains. $N = 100$.

As expected, the orientation factor f_1 (Fig. 1) assumes larger values for larger elongation ratio λ_1, but its values are reduced by elongation in the perpendicular direction λ_3. The decrease with increasing λ_3 is stronger at higher deformations λ_1 and λ_3. The tendency to level off the plots is seen when the deformation approaches its physical bounds given by the above inequality.

Negative values of the orientation factors indicate domination of perpendicular orientation. It is predicted that perpendicular alignment of segments (f_1 negative) can be produced by compression, $\lambda_3 < 1$. The stronger the compression, the higher is the stretch ratio λ_1.

As evident from Fig. 2, the orientation factor f_3 increases monotonically with increasing stretch ratio λ_3 in the extension, as well as in the compression ranges. At the same time, f_3 is reduced by perpendicular stretching, $\lambda_1 > 1$. Comparison of slopes of the plots shown in Figs. 1 and 2 indicate stronger effect of the stretch deformation λ_3 on the orientation factor f_3 than on f_1. Similar conclusion was found for infinitesimally small biaxial deformations in the series expansion model [17].

Tendencies in the behavior of the axial orientation factors in biaxial deformation predicted in our paper and by the series expansion theory [17] are generally in a qualitative agreement. However, the results shown in Ref. [17] are limited to first- and second-order approximation in the computations, and indicate significant differences between different levels of approximation, in particular at high

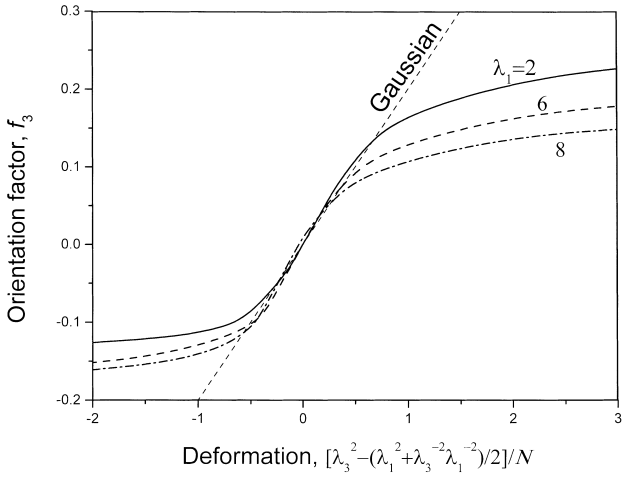

Fig. 3. Axial orientation factor f_3 vs. deformation $[\lambda_3^2/N - (\lambda_1^2 + \lambda_1^{-2}\lambda_3^{-2})/2]/N$ at fixed values of the elongation ratio λ_1 (indicated) computed from Eq. (60) for biaxial affine deformation of Gaussian and non-Gaussian chains. $N = 100$.

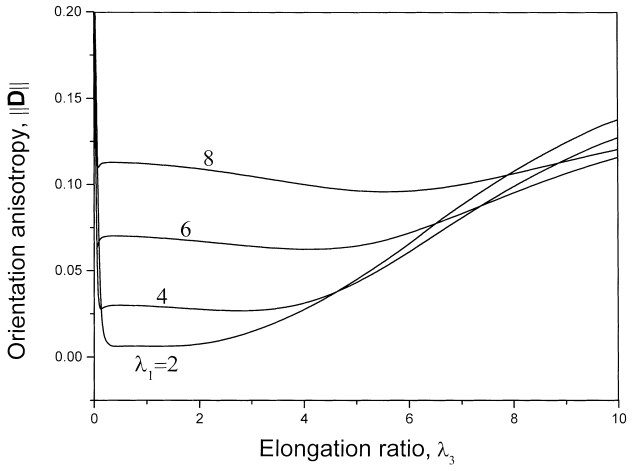

Fig. 4. Global orientation anisotropy characteristic $\|\mathbf{D}\|$ vs. elongation ratio λ_3 at fixed values of the elongation ratio λ_1 (indicated). Computed from Eq. (62) for biaxial affine deformation of non-Gaussian chains. $N = 100$.

deformations. For example, convergence of the axial orientation factor f_3 in Ref. [17] to the same value at different transversal extensions λ_1, with increasing λ_3, seems to be an artifact of the second-order approximation. Such a convergence is not predicted by our model (see Fig. 2). Such an uncertainty related to different behavior at different levels of approximation does not concern the closed-formula approach.

The plot of f_3 vs. $[\lambda_3^2 - (\lambda_1^2 + \lambda_1^{-2}\lambda_3^{-2})/2]/N$ shown in Fig. 3 reveals deviation of the predictions based on Gaussian statistics from the more general non-Gaussian relation. The linear single Gaussian plot for any λ_1, λ_3 pair splits in the case of non-Gaussian statistics into separate non-linear plots, at fixed λ_1 values. Significant deviation towards much smaller values of the orientation factor is observed for stretch ratios far from unity. However, within a range of small deformations, the non-Gaussian f_3 values exceed slightly the Gaussian once. Such a tendency in this deformation range is indicated by Eq. (70) where the first non-Gaussian correction term enhances values obtained from the linear one. At stronger deformations, the enhancement is compensated by higher order terms, and the obtained values drop below the Gaussian plot.

Global anisotropy of the system, characterized by the scalar characteristic $\|\mathbf{D}\|$, Eq. (62), is shown in Fig. 4. The plots indicate increase in the characteristic with increasing stretch ratio in the extension range where the extension exceeds the one in the transversal direction. Increase in the characteristic in this extension range is steeper at lower transversal extensions. This leads to intersections of each plot in Fig. 4 with the others of higher transversal extensions. The intersection indicates that effectivity of an extension in production of the overall anisotropy can be enhanced or weakened by the transversal extension. The enhancement takes place when the transversal extension does not exceed, and the reduction when it does exceed the current extension. The anisotropy characteristics are less sensitive to the extension in the first range, and they show very steep increase at strong compressions.

The average normal stress differences in biaxial deformation read

$$\langle \Delta p^{(3,1)} \rangle \equiv \langle p_{33} \rangle - \langle p_{11} \rangle = \frac{kT}{Nv_0}\left(\lambda_3^2 - \lambda_1^2\right) + \frac{1}{5}\frac{kT}{N^2 v_0}\left(3\lambda_3^4 - \frac{1}{\lambda_3^2} - 3\lambda_1^4 + \frac{1}{\lambda_1^2}\right) + \mathrm{O}\left(\frac{1}{N^3}\right) \quad (75)$$

$$\langle \Delta p^{(3,2)} \rangle \equiv \langle p_{33} \rangle - \langle p_{22} \rangle = \frac{kT}{\mathrm{N}v_0}\left(\lambda_3^2 - \frac{1}{\lambda_1^2\lambda_3^2}\right) + \frac{1}{5}\frac{kT}{N^2 v_0}\left(3\lambda_3^4 - \frac{3}{\lambda_1^4\lambda_3^4} + \lambda_1^2\lambda_3^2 - \frac{1}{\lambda_3^2}\right) + \mathrm{O}\left(\frac{1}{N^3}\right) \quad (76)$$

and for the uniaxial case

$$\langle \Delta p \rangle \equiv \langle p_{33} \rangle - \langle p_{11} \rangle = \frac{kT}{Nv_0}\left(\lambda_3^2 - \frac{1}{\lambda_3}\right) + \frac{1}{5}\frac{kT}{N^2 v_0}\left(3\lambda_3^4 + \lambda_3 - \frac{4}{\lambda_3}\right) + \mathrm{O}\left(\frac{1}{N^3}\right) \quad (77)$$

Figs. 5 and 6 show the average normal stress differences, $\langle \Delta p^{(3,1)} \rangle$ and $\langle \Delta p^{(3,2)} \rangle$ plotted vs. elongation ratio λ_3, at different fixed values of λ_1. The plots are computed using non-Gaussian distribution of end-to-end vectors. The stress differences monotonically increase with increasing elongation ratios. The biaxial stress difference between the two stretch directions, $\langle \Delta p^{(3,1)} \rangle$, is stronger than the stress difference $\langle \Delta p^{(3,2)} \rangle$ in the plane perpendicular to the deformation plane.

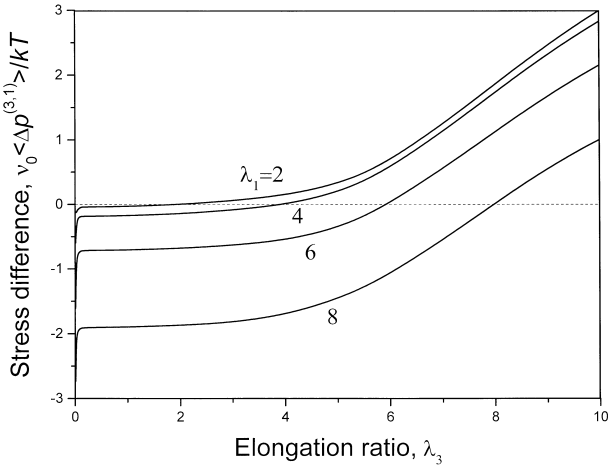

Fig. 5. Reduced normal stress difference, $v_0\langle\Delta p^{(3,1)}\rangle/kT$, vs. elongation ratio λ_3, at fixed values of the elongation ratio λ_1 (indicated). Computed from Eq. (52) with the non-Gaussian distribution of chain end-to-end vectors, Eq. (42), and the Padé approximation. $N = 100$.

Gaussian statistics imply normal stress difference proportional to the difference of deformation coefficients, λ_i^2/N:

$$\frac{\langle\Delta p^{(i,j)}\rangle v_0}{kT} = \frac{1}{N}\left(\lambda_i^2 - \lambda_j^2\right) \tag{78}$$

The Gaussian approximation converges with the non-Gaussian one in the range of elongation or compression ratios close to unity.

For Gaussian statistics, the relation between the average anisotropy tensor and the deviator of the average stress tensor is linear

$$\mathbf{D} = \frac{1}{5}\frac{v_0}{kT}\mathrm{dev}\langle\mathbf{p}\rangle = \frac{1}{5}\frac{v_0}{kT}\mathbf{P} \tag{79}$$

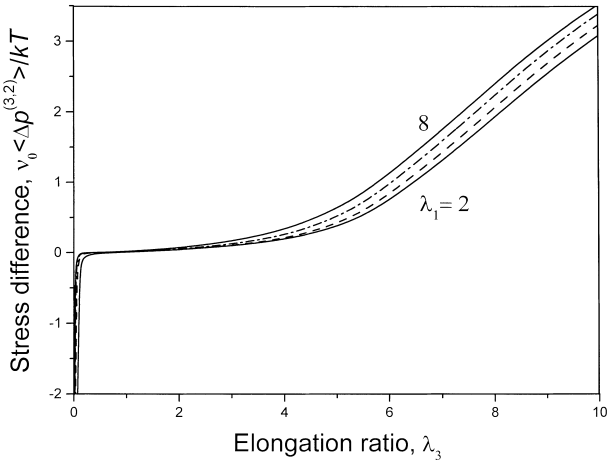

Fig. 6. Reduced normal stress difference, $v_0\langle\Delta p^{(3,2)}\rangle/kT$, vs. elongation ratio λ_3, at fixed values of the elongation ratio λ_1 (indicated). Computed from Eq. (52) with the non-Gaussian distribution of chain end-to-end vectors. $N = 100$.

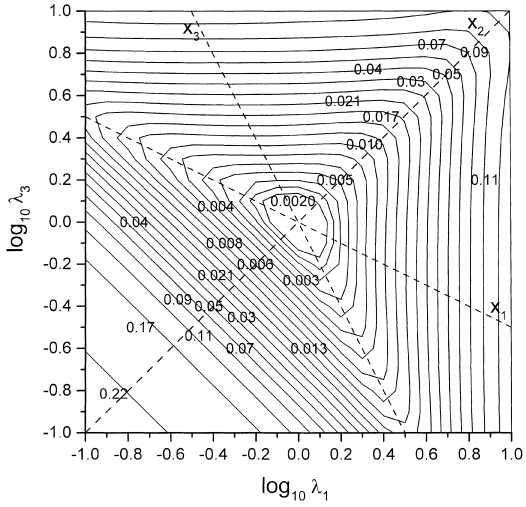

||**D**||

Fig. 7. The map of global orientation anisotropy characteristic, $\|\mathbf{D}\|$, in the space of biaxial deformations. Straight dashed lines indicate points of uniaxial deformation corresponding to, respectively, x_1, x_2, and x_3-axes.

and

$$f_3 = \frac{1}{5}\frac{v_0}{kT}\left[\langle p_{33}\rangle - \frac{1}{2}(\langle p_{11}\rangle + \langle p_{22}\rangle)\right]$$

$$= \frac{1}{10}\frac{v_0}{kT}(\langle\Delta p^{(3,1)}\rangle + \langle\Delta p^{(3,2)}\rangle) \tag{80}$$

The map of global orientation anisotropy $\|\mathbf{D}\|$ in the plane of variables λ_1, λ_3 of isochoric biaxial deformation ($\lambda_1\lambda_2\lambda_3 = 1$) is shown in Fig. 7, and the map of stress anisotropy $\|\mathbf{P}\|$ in Fig. 8. Straight dashed lines in the figures indicate points of uniaxial deformation along x_1, x_2, or x_3-axis. The maps are symmetrical with respect to the line $\lambda_1 = \lambda_3$ which corresponds to uniaxial stretch (or compression) along x_2-axis.

A characteristic feature of the maps is nearly constant

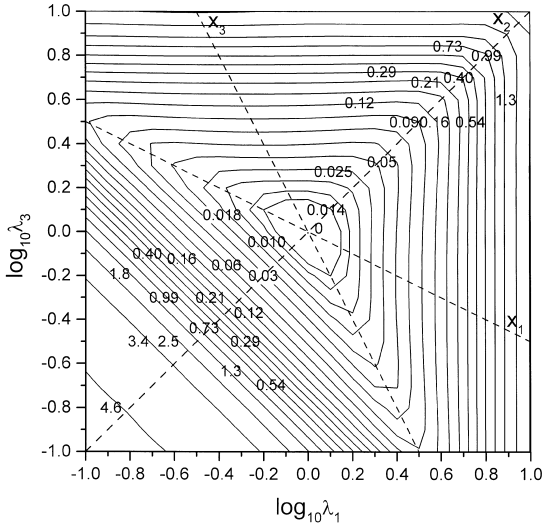

||**P**||

Fig. 8. The map of global dimensionless stress anisotropy, $v_0\|\mathbf{P}\|/kT$, in the space of biaxial deformations. For dashed lines see Fig. 7.

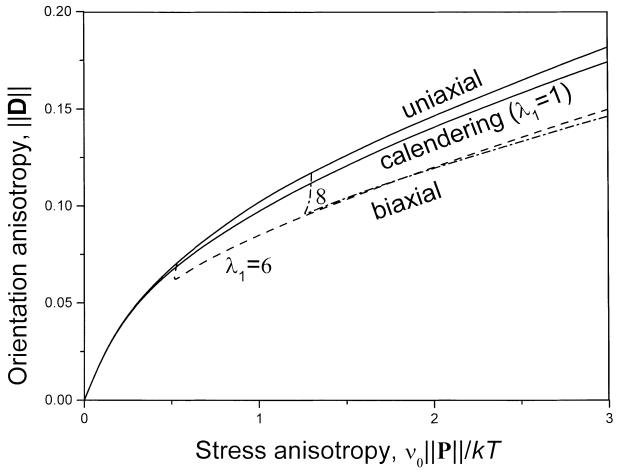

Fig. 9. Global orientation–stress anisotropy in uniaxial stretch, calendering, and biaxial deformation at fixed stretch ratios (indicated).

global stress and orientation anisotropy in the entire range of stretch ratio λ_i, at fixed stretch ratio in the perpendicular direction, $\lambda_j = \text{const}$, providing that $\lambda_i < \lambda_j$. At the point of equal stretches, $\lambda_i = \lambda_j$, the anisotropy behavior changes and with increasing λ_i above the fixed λ_j value, the anisotropy characteristics monotonically increase. Global anisotropy increases with increasing stretch ratio along the direction of dominating stretch, $\lambda_i > \lambda_j$. Such a behavior does not concern calendering, $\lambda_i = 1$.

In the case of uniaxial deformation or calendaring, where the deformation lines traverse the point $\lambda_1 = \lambda_2 = \lambda_3 = 1$, monotonic increase of the global anisotropies $\|\mathbf{D}\|$ and $\|\mathbf{P}\|$ with increasing deformation is predicted, without any range of flattening.

Uniaxial stretch provides the highest orientational response to the stress, as shown in Fig. 9. Calendering, $\lambda_1 = 1$, although less effective than the uniaxial deformation, dominates the biaxial deformation at $\lambda_1 > 1$. Both deformations, uniaxial stretch and calendering, show a non-linear, monotonic increase in the orientation anisotropy with increasing stress anisotropy.

Such a monotonic behavior is disturbed for biaxial deformations at the fixed stretch ratio exceeding unity, $\lambda_1 > 1$. This is clearly shown in Fig. 9 in the case of $\lambda_1 = 6$ and 8. Monotonic increase of these plots starts from the point of equal stretch ratios. For stretch ratio below the fixed λ_1 value, the orientation–stress anisotropy relation concerns much narrower stress anisotropy range, and shows quite a different behavior. Within this range, stress anisotropy and orientation anisotropy both decrease with increasing stretch ratio λ_3, and at the point of equal stretches, $\lambda_3 = \lambda_1$, merge the line of monotonic increase.

7. Conclusions

Axial orientation factor increases monotonically with axial stretching, and it is reduced by transversal stretching (λ_3 reduces with λ_1, and vice versa). Axial stretching is more effective for axial segmental orientation than the transversal one.

Maps of global orientation and stress anisotropy in biaxial deformation indicate nearly constant values of both characteristics in the range of stretch ratios not exceeding the stretch ratio in the transversal direction. Roles of the deformation ratios change at the point of equivalence. By increasing the stretch ratio above that in the transversal direction, a non-linear, monotonic increase in the anisotropy characteristic is predicted.

Any application of transversal stretching reduces the anisotropy continuously, from the uniaxial deformation geometry, throughout calendering, up to any perpendicular stretch ratio above unity.

Difference of normal stresses between the two stretch directions is stronger than the stress difference in the perpendicular free plane. Both stress differences monotonically increase with increasing elongation ratios.

Gaussian chain statistics imply normal stress differences proportional to the difference of square deformation ratios reduced by the number of segments in a chain, $(\lambda_j^2 - \lambda_i^2)/N$, and the relation between the average tensors of orientation and stress is linear.

Significant deviation of stresses from the Gaussian model are predicted at higher deformations, and convergence to Gaussian behavior is seen in a relatively narrow range of small stresses and deformations.

Acknowledgements

This work was supported in part by Dow Chemical Co., Midland, Michigan. Preliminary results were presented before the SPE-RETEC Symposium ‘Orientation of Polymers’, Boucherville, Canada [22].

References

[1] Ziabicki A. In: Happey F, editor. Applied fibre science, vol. III. New York: Academic Press, 1979. p. 257.
[2] Ziabicki A, Kedzierska K. J Appl Polym Sci 1962;6:111, see also p. 361.
[3] Nishijima Y, Onogi Y, Assai T. J Polym Sci 1966;15:237.
[4] Nishijima Y. J Polym Sci 1970;31:353.
[5] Kashiwagi M, Cunningham A, Manuel AJ, Ward IM. Polymer 1973;14:111.
[6] Cunningham A, Ward IM, Willis HA, Zichy V. Polymer 1974; 15:749.
[7] Jarvis DA, Hutchinson IJ, Bower DI, Ward IM. Polymer 1980;21: 41.
[8] Jabarin SA. Polym Engng Sci 1984;24:376.
[9] Ward IM. Adv Polym Sci 1985;66:81.
[10] Bower DI, Jarvis DA, Ward IM. J Polym Sci, Polym Phys Ed 1986;24:1459.
[11] Hendrichs PM. Macromolecules 1987;20:2099.
[12] Lapersone P, Tassin JF, Sergot P, Monnerie L, Bourvellec GL. Polymer 1989;30:1558.
[13] Cakmak M, Kim JC. J Appl Polym Sci 1997;65:2059.

[14] Kim JC, Cakmak M, Zhou X. Polymer 1998;39:4225.
[15] Sugimoto M, Masubuchi Y, Takimoto J, Koyama K. Macromolecules 2001;32:6056.
[16] White JL, Spruiell JE. Polym Engng Sci 1981;21:850.
[17] Sarac Z, Erman B, Bahar I. Macromolecules 1995;28:582.
[18] Nagai K. J Chem Phys 1964;40:2818.
[19] Cohen A. Rheol Acta 1991;30:270.
[20] Kuhn W, Grün F. Kolloid Z 1941;95:172, see also p. 307.
[21] Zimm BH. J Chem Phys 1956;24:269.
[22] Ziabicki A, Jarecki L. Molecular orientation in biaxially deformed polymers. SPERETEC Symposium Orientation of Polymers. Boucherville, Canada, September 1998.